

## **Design of Waterborne Nanoceria/Polymer Nanocomposite UV-Absorbing Coatings: Pickering *versus* Blended Particles**

Ignacio Martín-Fabiani,<sup>1,\*</sup> Ming Liang Koh,<sup>2</sup> Florent Dalmas,<sup>3</sup> Katrin L. Elidottir,<sup>4</sup> Steven J. Hinder,<sup>5</sup> Izabela Jurewicz,<sup>4</sup> Muriel Lansalot,<sup>2</sup> Elodie Bourgeat-Lami<sup>2</sup> and Joseph L. Keddie<sup>4</sup>

<sup>1</sup> *Department of Materials, Loughborough University, Loughborough LE11 3TU, Leicestershire, United Kingdom*

<sup>2</sup> *Univ Lyon, Université Claude Bernard Lyon 1, CPE Lyon, CNRS, UMR 5265, Chemistry, Catalysis, Polymers & Processes (C2P2), 43 Bd du 11 Novembre 1918, 69616 Villeurbanne, France.*

<sup>3</sup> *Univ Lyon, INSA Lyon, CNRS, Material Science and Engineering (MATEIS) UMR 5510, 7 av J. Capelle, F-69621 Villeurbanne, France*

<sup>4</sup> *Department of Physics, University of Surrey, Guildford GU2 7XH, United Kingdom*

<sup>5</sup> *Surface Analysis Laboratory, Department of Mechanical Engineering Sciences, University of Surrey, Guildford GU2 7XH, United Kingdom*

\*i.martin-fabiani@lboro.ac.uk

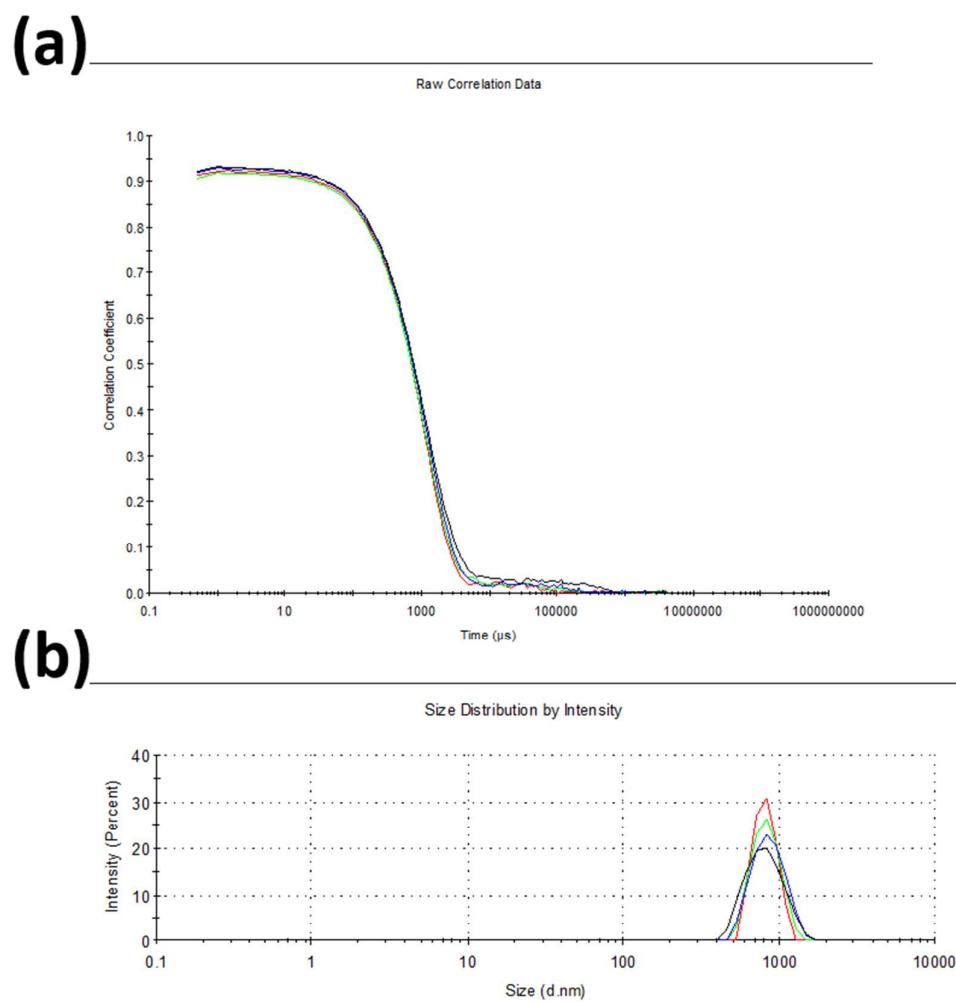


**Figure S1.** DLS correlograms (a) and particle size distributions (b) for the SFB latex.

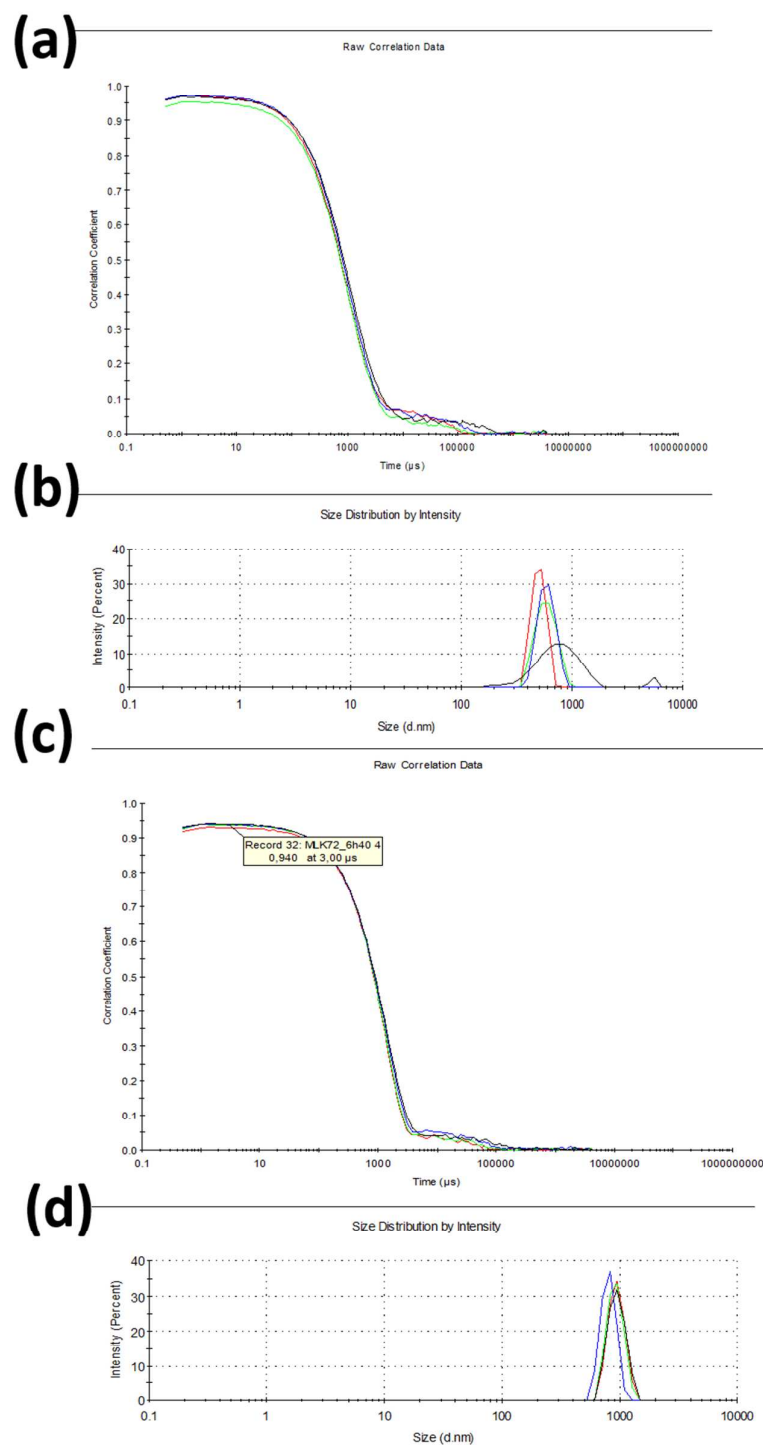


**Figure S2.** DLS correlograms (a) and particle size distributions (b) for the ACS Pickering latex. DLS correlograms (c) and particle size distributions (d) for the BCS Pickering latex.

### **Atomic force microscopy of Pickering particles**

Atomic force microscopy (using an Ntegra atomic force microscope, NT-MDT, Moscow) was performed to provide information about the particle sizes and distributions of the ACS and BCS particles to complement the DLS. Latex particle layers were deposited by dropping a small amount of dispersion onto a cleaved mica substrate, before spin-coating at 4000 r.p.m. for 10 seconds to remove any excess liquid. AFM measurements were taken immediately. Results are presented in Figure S3. After sampling 60 particles per sample, the analysis yields a mean size of  $540 \pm 85$  nm for ACS particles and  $950 \pm 120$  nm for BCS particles. Analysis of cryo-TEM images finds a value of particle size of approximately 450 nm for ACS particles and 900 nm for BCS particles.

In summary, size measurements obtained by DLS, cryo-TEM and AFM are in broad agreement and confirm that that BSC particles are approximately twice the size of the ACS particles. The cryo-TEM measurements are lower than the AFM measurements probably because there is some spreading of the particles on the mica substrates. As DLS measures the hydrodynamic radius, this technique finds a slightly larger value than the microscopy measurements.

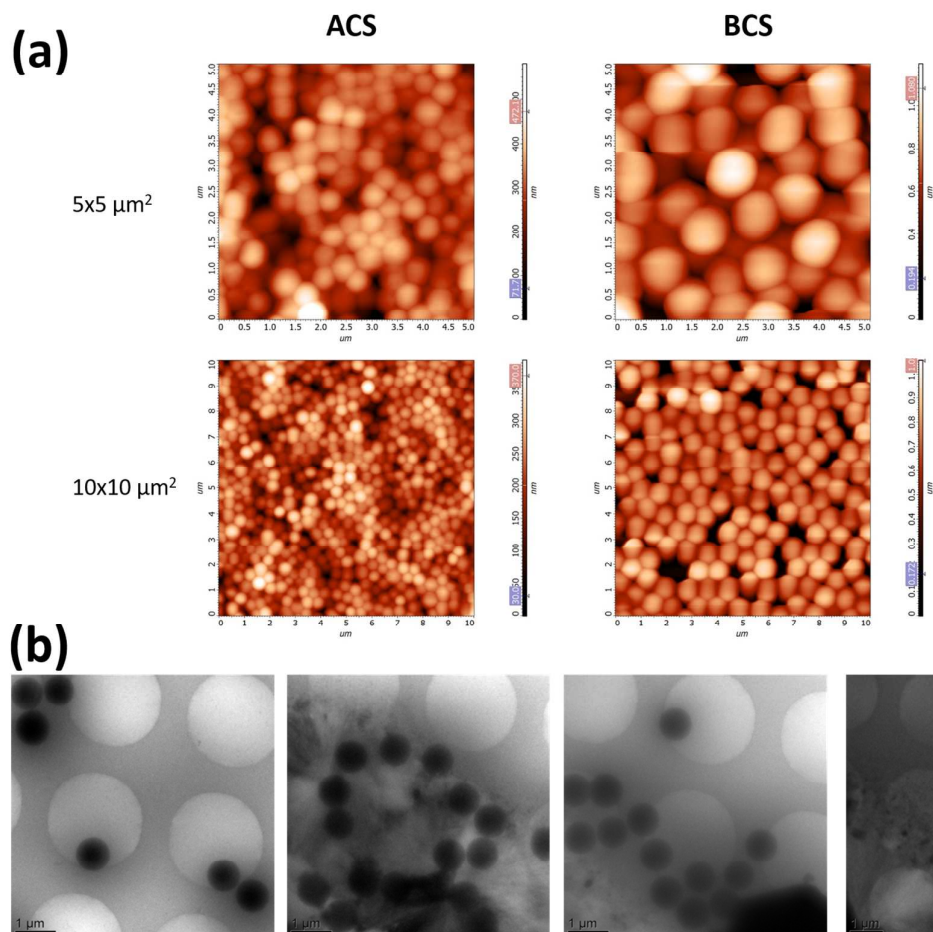


**Figure S3.** (a) Atomic force microscopy topographic images obtained from ACS Pickering particles (left column) and BSC Pickering particles (right column) over areas of  $5 \times 5 \mu\text{m}^2$  (first row) and  $10 \times 10 \mu\text{m}^2$  (second row). (b) Cryo-TEM images of BCS Pickering particles. The nanocomposite particles appear as dark circles. The scale bar is 1  $\mu\text{m}$  in all images.

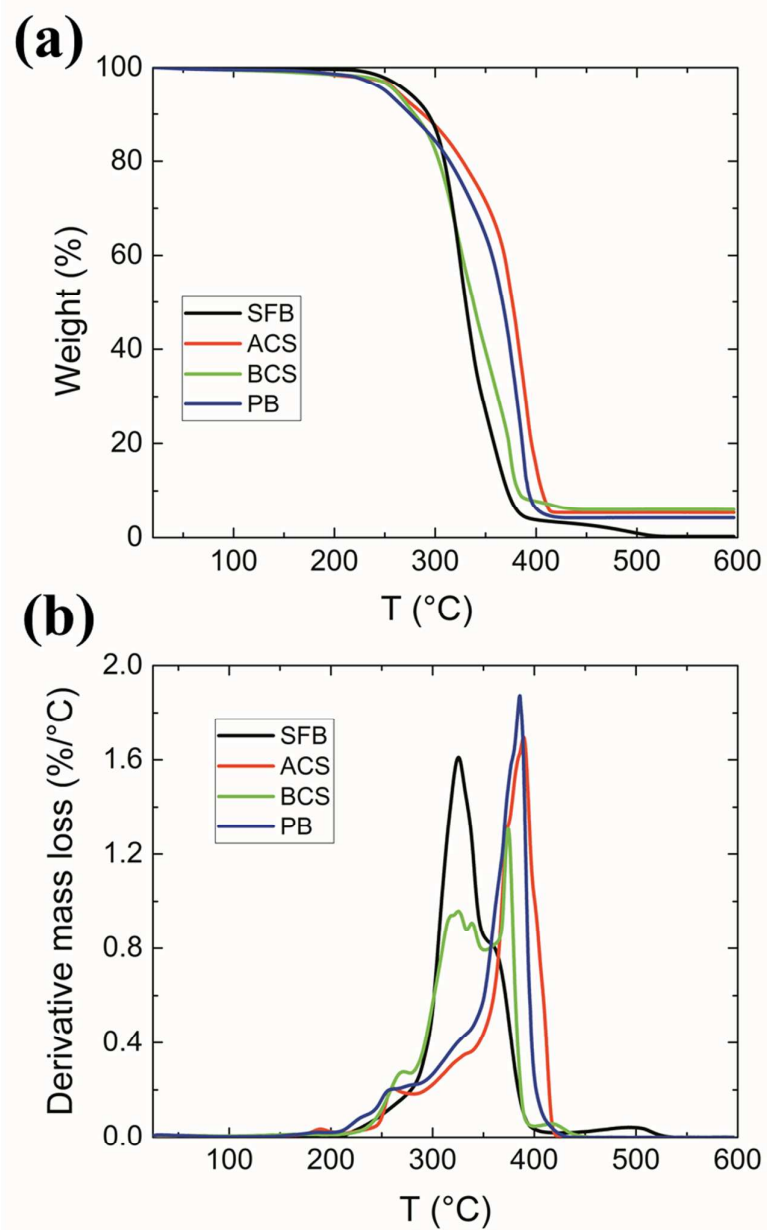


**Figure S4.** Thermogravimetric analysis of the blank latex, the physical blend and the ceria stabilized latexes: (a) mass loss and (b) derivative mass loss as a function of temperature.

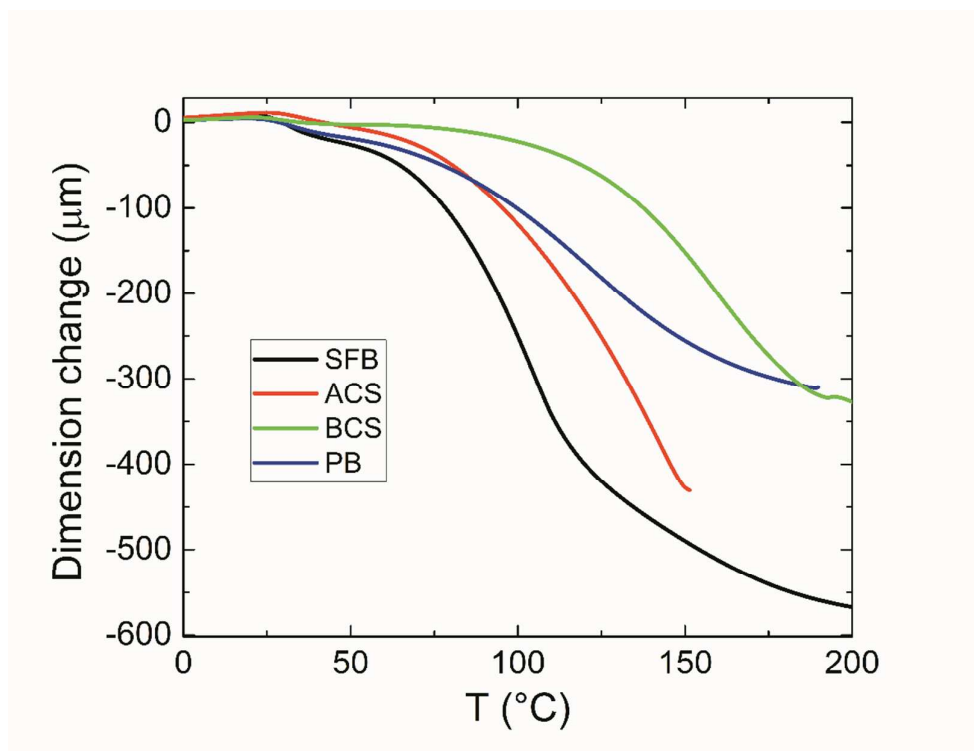


**Figure S5.** Dimensional change as a function of temperature for the blank latex, the physical blend and the ceria stabilized latexes as determined by TMA. Data are shown up to the temperature at which the measurement became unstable.

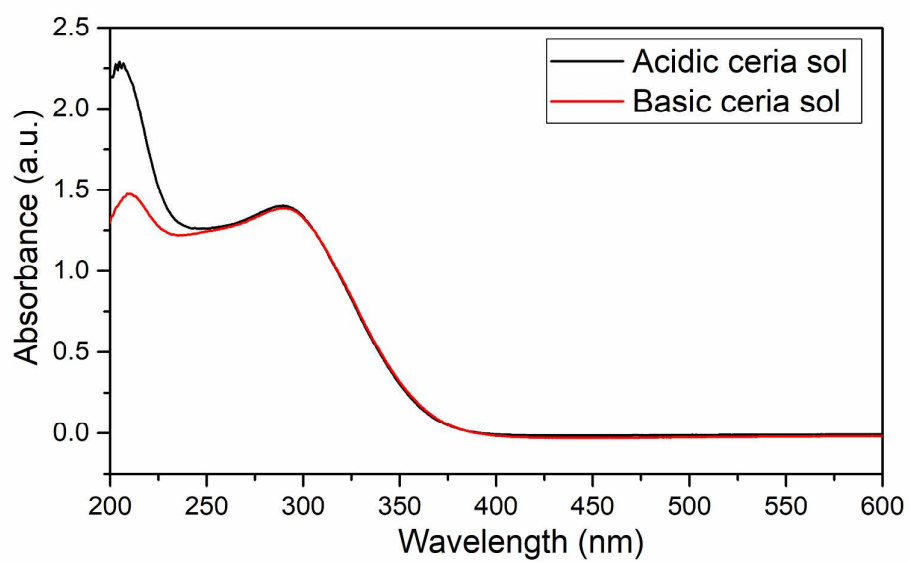


**Figure S6.** Absorbance spectra obtained for the acidic and basic ceria sol after dilution by 400 times in deionized water.



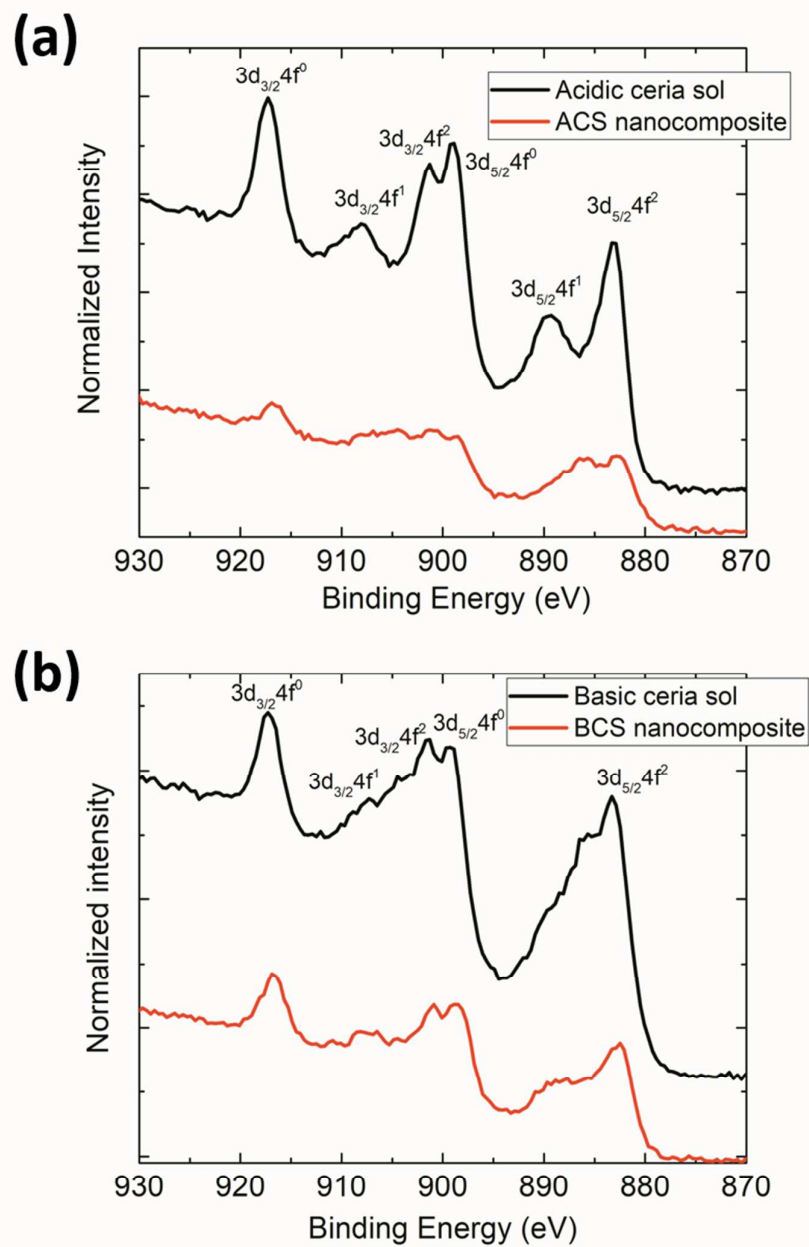


**Figure S7.** Ce 3d spectra of (a) ACS and (b) BCS nanocomposites as obtained by XPS (red lines) compared to the same spectra obtained from the corresponding sol nanoparticles (black lines).

**Table S1.** Elemental surface analysis of the ceria sol nanoparticles and their nanocomposites determined by XPS

	<b>Atomic %</b>			
<b>Element and Orbital</b>	<b>Acidic ceria sol nanoparticles</b>	<b>Basic ceria sol nanoparticles</b>	<b>ACS Nanocomposite</b>	<b>BCS Nanocomposite</b>
C 1s	30.0	42.9	46.4	49.9
Ce 3d	11.7	9.7	1.5	3.3
N 1s	6.7	2.1	6.5	1.0
O 1s	51.7	42.7	34.1	34.4

The presence of N in the acidic ceria sol nanoparticles and nanocomposite is attributed to the presence of  $\text{NO}_3^-$  (from nitric acid). The higher C:Ce ratio in the basic ceria sol nanoparticles and nanocomposites is attributed to the presence of citric acid on the nanoceria surface.

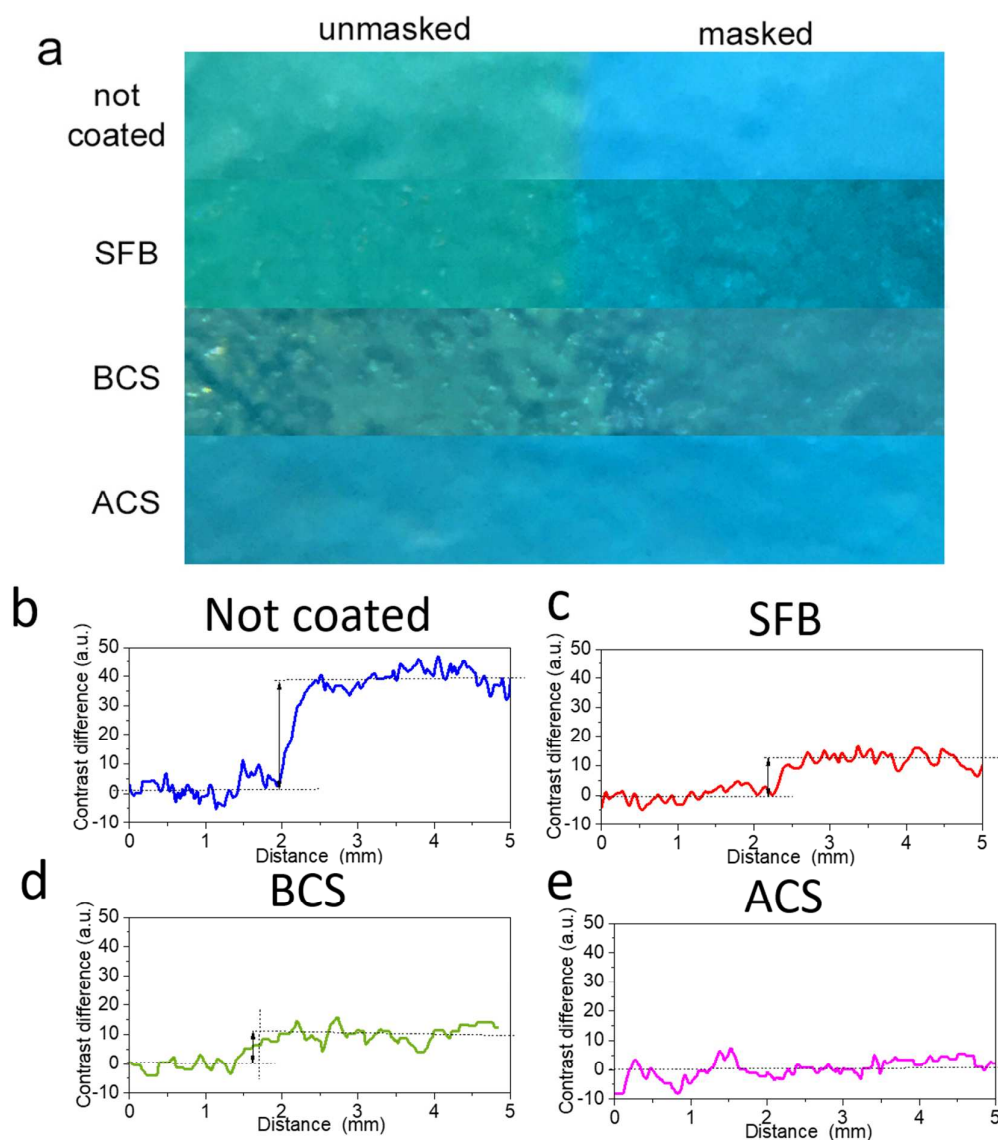


**Figure S8.** (a) Optical micrographs of the unmasked and masked regions of the poly(chloroprene) rubber substrate after UV irradiation coated with different latexes. Contrast profiles across the masked/unmasked boundary after UV irradiation for (b) coloured rubber film and the same film coated with (c) SFB, (d) BCS and (e) ACS.